

MULTI-TEMPORAL PIXEL TRAJECTORIES OF SAR BACKSCATTER AND COHERENCE IN TROPICAL FORESTS

Elsa Carla De Grandi¹, Edward Mitchard², Dirk Hoekman³, Astrid Verhegghen⁴, Francesco Holecz⁵ and Paula Nieto Quintano⁶

1. University of Edinburgh, School of GeoSciences, Edinburgh, United Kingdom; E.De-Grandi@sms.ed.ac.uk.
2. University of Edinburgh, School of Geosciences, Edinburgh, United Kingdom; edward.mitchard@ed.ac.uk.
3. Wageningen University, Wageningen, The Netherlands; dirk.hoekman@wur.nl.
4. Joint Research Center, Ispra, Italy; astrid.verhegghen@jrc.ec.europa.eu.
5. Sarmap, Cascine di Barico, Switzerland; fholecz@sarmap.ch.
6. University of Edinburgh, School of GeoSciences, Edinburgh, United Kingdom; paula.nieto@ed.ac.uk

ABSTRACT

Tropical forest natural and anthropogenic changes can be tracked using a pixel based time-series analysis of multi-temporal Interferometric Synthetic Aperture Radar (InSAR) backscatter and coherence provided by TanDEM-X. A pixel trajectory is defined as a set of values of all resolution elements (backscatter or coherence) at the same row and column position in the stack of images. Analysis of the trajectories over an area by means of a set of parameters (features) that characterize its time evolution can give insight on the nature and changes of tropical forest due to disturbance events (e.g. deforestation) but also due to natural changes in environmental conditions (e.g. rainfall). The following set of trajectory features was computed: linear fitting (trend), dispersion around trend (RMSE), maximum change (swing), statistics of the trajectory finite difference at one step (variance and intermittency). Results indicate that linear regression parameters captured changes due to forest/non forest conversion. The study reports results from a highly disturbed tropical forest environment in the Republic of Congo.

INTRODUCTION

The Congo Basin hosts the second largest dense humid tropical forest in the world after the Amazon rainforest playing a crucial role in the global climate system. Mapping tropical forests is a requirement for international initiatives such as Reducing Emission from Deforestation and Forest Degradation (REDD+). This can be best achieved using Synthetic Aperture radar such as TanDEM-X. TanDEM-X coherence can improve the separability between thematic classes as it is modulated by the volume through decorrelation and this depends on forest canopy scatterers and can be linked to canopy structure (e.g. canopy cover) (1). We present results from a site located in the Sangha Department (Republic of Congo) which covers 25 x 40 km (Figure 1). Clearing of secondary forest around urban centers is extensive for shifting cultivation (2). The Ngombe and Pokola logging concession were also situated in the study site where, exploitation of forest through selective logging was undertaken between 1985 and 2008.

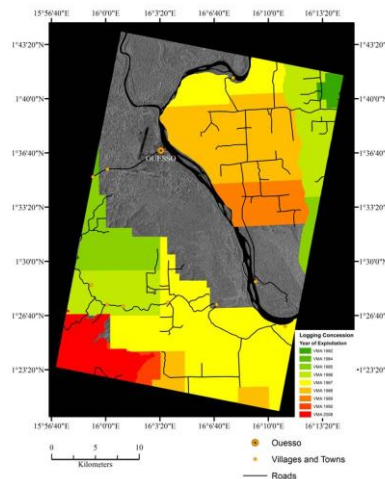


Figure 1: Study site location in the Sangha Department, Republic of Congo (RoC). Data Source: World Resources Institute (WRI) and DLR.

METHODS

Dataset and Processing

Six TanDEM-X StripMap scenes (supplied by DLR through the VEGE03030 AO) were acquired between 2012 and 2014, at HH polarization, 47° incidence angle and descending mode (Table 1). The data was processed using SARscape software (5.0) (3) and included the following steps: a) multi-looking (2 range and 2 azimuth looks, corresponding to a slant range pixel size of 3.69 x 3.73 m); b) interferometric workflow (interferogram generation and flattening, adaptive local frequency filter and coherence generation); c) co-registration d) multi-temporal filtering e) geocoding in a Geo-Global Lat/Lon system with $3.33 \cdot 10^{-5}$ degree pixel size (approximately 4 m). Both the backscatter (power) and the coherence datasets were co-registered and filtered to reduce noise (speckle and coherence estimator variance) using the multi-temporal filter implemented in SARscape and based on the principle proposed in (4). Very High Resolution data acquired in December 2013 available from Google Earth (Figure 2), and accumulated precipitation data from Tropical Rainfall Measuring Mission (TRMM) were used as reference data. Visual interpretation of the reference datasets was used for training the supervised analysis by selecting 15x15 pixels Areas Of Interest (AOI). Selected thematic classes are: lowland forest, swamp forest, agriculture and grassland. It is important to note, in the context of the time-series analysis performed in this work that the class definition corresponds to the situation at t_4 , which is the date of the available Google Earth dataset with the highest spatial resolution.

Table 1: Multi-temporal stack used to compute multi-temporal pixel trajectories.

Time	Date	Baseline (m)	Rainfall (mm)*
t1	05/12/2012	95.3	0
t1	14/03/2013	24.5	0.587
t3	19/05/2013	24.5	20.657
t4	25/12/2013	52	7.603
t5	03/04/2014	111.2	29.843
t6	06/05/2014	63	12.382

*based on TRMM data for a period of a 48 h before the date of acquisition.

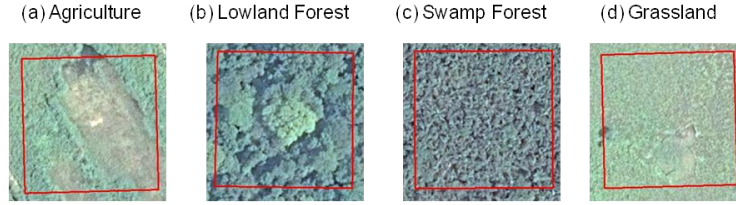


Figure 2: Areas of Interest (AOI) used for the analysis on Very High Resolution Google Earth imagery acquired on December 17th, 2013 (Data Source: Google Earth, 2013).

Multi-temporal Pixel Trajectories

A pixel trajectory is defined as a set of values of all resolution elements at the same row and column position in the stack of images. The following set of trajectory features were computed on either the multi-temporal backscatter stack or multi-temporal coherence: a) Trend analysis by linear regression (line intercept, slope and deviations from the trend); b) Swing c) Variance of the de-trended trajectory's finite differences at 1 step and d) Maximum of the absolute value of the finite difference vector.

a) Trend analysis by linear regression of $P_j (j = 1..n)$, where P is the pixel value at date j , n is the number of dates in the multi-temporal stack. This step yields the fitting line with two parameters (slope m and intercept c), and the root mean squared deviations of the points from the line (rms):

$$y(k) = c + m k \quad (1)$$

$$\nabla Prms = \sqrt{\sum_{k=1}^n (P(k) - y(k))^2} \quad (2)$$

b) Swing:

$$\max(P_j) - \min(P_j) \quad (3)$$

c) Variance of the de-trended trajectory's finite differences at 1 step (a measure of departure velocity from trend) :

$$Pdt(k) = P(k) - y(k) \quad (4)$$

$$d(k) = Pdt_{k+1} - Pdt_k \quad (5)$$

$$VD = \log \left(\frac{1}{n-1} \sum_{k=1}^{n-1} d^2(k) - \left(\frac{1}{n-1} \sum_{k=1}^{n-1} d(k) \right)^2 \right) \quad (6)$$

d) Maximum of the absolute value of the finite difference vector (a measure of large intermittent events):

$$Md = \text{Max}(d(k)) \quad (7)$$

RESULTS

Multi-temporal Pixel Trajectories of SAR Backscatter

Results indicate that multi-temporal pixel trajectories pick up changes related to: (i) environmental conditions (seasonality and rainfall) and (ii) forest disturbance (e.g. deforestation).

Mean Radar Cross Section (RCS) for four AOI indicates that the variations for lowland forest and swamp forest are not as marked as those for agriculture and grassland (Figure 3). The changes in lowland forest and swamp forest can be mainly attributed to changes due to environmental effects (e.g. moisture) and not due to anthropogenic disturbance such as clearing.

Lowland forest presents high RCS throughout the time series with no significant sign of disturbance since the area is situated far from the main villages and towns, outside of the logging concessions. However, there is a noticeable fluctuation in RCS for this class due to rainfall events, these changes being all < 1dB. Swamp forest also presents small fluctuations in RCS (<1dB), these being also attributable to the impact of environmental conditions. Given the canopy density of both forest types, the extinction at X-band is large (penetration small), which makes the average return similar over areas comprising several crowns. Whereas, at shorter scales (e.g. a few meters) more RCS variation is expected for the less homogeneous lowland forest.

Greater change in RCS is noticeable for the agriculture and grassland classes, this being a consequence of anthropogenic disturbance due to the proximity to urban areas and the increased accessibility to the area. A noticeable change in RCS for class agriculture is detected (highest RCS is -10.8 dB and lowest RCS is -19.2 dB). The grassland trajectory is similar in time development to the swamp forest one, but with overall lower RCS. This is in line with backscattering from a homogeneous vegetation layer, similar to the forest but with less scatterer number density. Grassland also undergoes changes especially between date 3 (-12.2 dB) with subsequent decrease to -14.3 dB at date 4. The high RCS is attributable to the presence of taller grass which is then cleared and converted into bare field in preparation for agriculture with the underlying influence of moisture conditions also contributing to the RCS (Figure 3d).

Analysis of multi-temporal pixel features within an AOI (Figure 4) provide extra information to understand the RCS dynamics (Table 2). The swing is highest for the class agriculture, because of a discontinuity at t_5 (decrease in backscatter) which is attributable to a change in terrain cover, with a transition from a surface with a vegetation layer, responsible of RCS similar to that of the forest areas, to a state of bare and smooth soil (Figure 3a).

Instead, the swing for both the lowland forest and the swamp forest is the lower. This feature indicates that the most dynamic classes are agriculture and grassland. The slope of the linear fit line also suggests that the trend in the class agriculture is very strong and negative (-60.9) while, the slope for the other 3 classes is positive with swamp forest having the lowest slope (1.1). The rms is highest for the class agriculture (1.7) and lowest for the lowland forest class (0.25). The variance of the finite differences is much higher for the class agriculture (10.5) compared to all the other classes. The same applies to the maximum absolute value of the differences (intermittency).

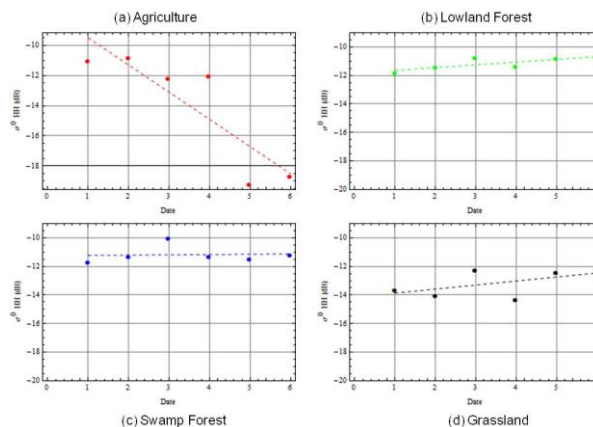


Figure 3. Radar Cross Section (RCS) linear regression for four AOI.

Table 2: Backscatter multi-temporal features statistics (mean) for four AOI (a) agriculture; (b) lowland forest; (c) swamp forest and (d) grassland.

Feature	(a)	(b)	(c)	(d)
Swing	8.3	1.1	1.6	2.0
Trend Slope	-60.9	10.9	1.1	15.7
Deviations from trend (rms)	1.7	0.2	0.5	0.7
Variance	10.5	0.2	0.9	2.6
Intermittency	29.0	0.5	1.7	5.2

Multi-temporal Pixel Trajectories of Coherence

Analysis of coherence for the same AOI revealed interesting trends (Figure 4 and 5). Coherence for class agriculture reveals that this is high until t_5 (0.72) (04/2014) where a sharp discontinuity occurs (this is in line with the RCS trajectory). The drop in coherence signals the passage from a vegetation layer with volume decorrelation similar to that of grassland and forest, to bare soil, where decorrelation is attributable to the spatial heterogeneity in the dielectric properties of soil (moisture) (5). Lowland forest presents coherence which is lower than all the other classes apart at t_2 where it is slightly above coherence for class grassland and at t_5 (04/2014) and t_6 (05/2014) where the class agriculture presents very low coherence. Lower coherence for lowland forest is to be expected, this is attributed to the spatially varying vertical structure (more heterogeneous canopy), calling for gaps and shadowing which modulate the volume decorrelation. Instead, swamp forest has a much more homogeneous canopy cover with smaller tree crowns and therefore, coherence is almost always higher compared to other classes.

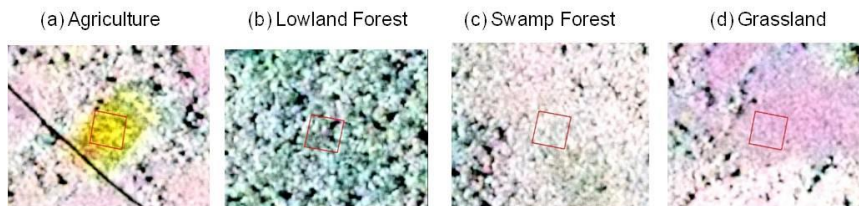


Figure 4: TanDEM-X coherence ($R= 12/2012$, $G= 12/2013$ and $B= 05/2014$) for four 15 x 15 pixel AOI. (a) agriculture; (b) lowland forest; (c) swamp forest and (d) grassland.

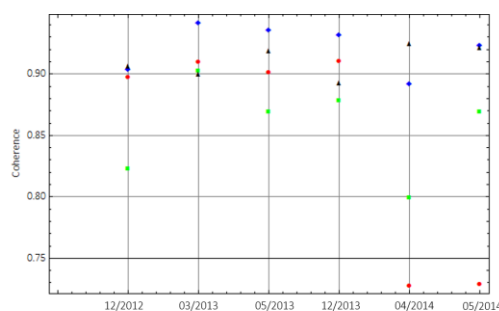


Figure 5: TanDEM-X coherence trajectory from December 5th, 2012 to May 6th, 2014 for (a) agriculture (red); (b) lowland forest (green); (c) swamp forest (blue) and (d) grassland (black).

Coherence multi-temporal features provide additional information to coherence trajectories over time within the AOI (Table 3). The results are in line with those reported about features of RCS trajectories.

Table 3: Coherence multi-temporal features statistics (mean) for four AOI (a) agriculture; (b) lowland forest; (c) swamp forest and (d) grassland.

Feature	(a)	(b)	(c)	(d)
Swing	0.18	0.10	0.049	0.031
Trend Slope	-2.25	-0.11	-0.09	0.20
Deviations from trend (rms)	0.049	0.034	0.017	0.010
Variance	0.0069	0.0046	0.0009	0.0005
Intermittency	0.0204	0.0067	0.0015	0.0009

CONCLUSIONS

Results indicated that multi-temporal pixel trajectories using TanDEM-X InSAR data are a useful tool to follow the evolution of natural targets. However, it is important to distinguish between natural changes due to seasonality and environmental conditions (e.g. rainfall), as in the case of results provided for lowland tropical forest and swamp forest, and changes due to anthropogenic disturbance (conversion from forest to non-forest). It was found that the features are able to characterize for instance the conversion from forest to non-forest (deforestation). The slope of the linear trend indicates the magnitude of the change and whether the trend in backscatter is positive (vegetation regrowth) or negative trend (deforestation). The combination of RCS and coherence trajectories can be effective not only in detecting discontinuities in the ecosystem dynamics (such as those induced by human intervention, or intermittent natural events), but also to discriminate vegetation classes with a stationary evolution in time. The analysis will be extended in particular to look at areas which present a negative trend to provide estimates of deforestation.

ACKNOWLEDGEMENTS

The authors would like to thank DLR for the provision of TanDEM-X data through AO proposal VEGE03030. The authors would also like to acknowledge the University of Edinburgh and the School of GeoSciences for funding the project.

REFERENCES

- Schund, M, F von Poncet, D H Hoekman, S. Kuntz, C Schmullius, 2014. Importance of bistatic features from TanDEM-X for forest mapping and monitoring. Remote Sensing of Environment, 151: 16–26.
- LaPorte, N T, T S Lim, J Lemoigne, D Devers, M Honzák, 2004. Towards an Operational Forest Monitoring System for Central Africa. In: Land Change Science: Observing, Monitoring and Understanding Trajectories of Change on the Earth's Surface, edited by G Gutman, A C Janetos, C O Justice, E F Moran, J F Mustard, R R Rindfuss, D Skole, B L Turner II & M A Cochrane (Kluwer Academic Publishers, The Netherlands) 97-110.
- The SAR Guidebook. http://www.exelisvis.com/portals/0/pdfs/envi/SAR_Guidebook.pdf (last date accessed: May 20th 2015).
- De Grandi, G F, M Leysen, J S Lee & D Schuler, 1997. Radar reflectivity estimation using multiple SAR scenes of the same target: Technique and applications. In: Proceeding of the IEEE International Geoscience and Remote Sensing Symposium - A Science Vision for Sustainable Development (IGARSS, Singapore), 1047– 1050.
- Luo, X, G Askne, G Smith & P Dammert, 2001. Coherence Characteristics of Radar Signals from Rough Soil. Progress in Electromagnetics Research, PIER, 31:69-88.